RoboTrikke: A Novel Undulatory Locomotion System

Sachin Chitta† Peng Cheng* Emilio Frazzoli‡ Vijay Kumar†

† GRASP Laboratory
University of Pennsylvania
Philadelphia, PA 19104 USA
sachinc,kumar@grasp.upenn.edu

* Department of Computer Science
University of Illinois
Urbana, IL 61801 USA
pcheng1@cs.uiuc.edu

‡ Mechanical & Aerospace Engineering
University of California
Los Angeles, CA 90095 USA
frazzoli@ucla.edu

***Abstract*— In this paper we present a mathematical model of the TRIKKE, a human-powered scooter produced by Trikke Tech Inc. The Trikke is a three-wheeled, single-rider vehicle that can be propelled by a combination of cyclic motion of its handlebar and swaying motion of the rider. Commercial versions of the Trikke with a human rider are capable of speeds up to 18 mph on ¤at ground. We show that the TRIKKE can be modeled as a modi£edroller-racer with an unstable steering setup opposite to that of a bicycle. We show that the model of the TRIKKE reduces to the roller-racer in the absence of this steering arrangement. Furthermore, we prove that under certain conditions on the geometric parameters of the system, the TRIKKE and roller racer systems cannot be stopped after motion starting from rest using the steering control as the sole input. As a consequence, the ideal model is severely limited from the point of view of controllability. We demonstrate the validity of our model through comparison with experimental measurements on a small-scale robotic version of the TRIKKE.**

I. INTRODUCTION

The TRIKKE (Fig. 1) is a three-wheeled human-powered scooter produced by **Trikke Tech Inc.**[1]. It can be propelled by a single rider using a combination of swaying and cyclic inputs to the steering axis. The rider's feet never move from £xed footrests on the TRIKKE, and do not come into contact with the ground, thus there is no *pushing off* unlike in riding a skateboard or rollerblading. The TRIKKE can achieve a speed of 18 mph on ¤at ground. The rider starts out by turning the steering axis from side to side. The TRIKKE then starts moving in a sinusoidal manner. The motion then progresses with the rider *rocking* the steering axis from side to side. The motion can be further complemented by an appropriate weight transfer onto different feet corresponding to the direction in which the TRIKKE is instantaneously turning.

Systems using unconventional undulatory locomotion techniques have been widely studied in the recent past. This includes systems like the Snakeboard [10], the Variable Geometric truss [7], the Roller Racer [8], the Roller Walker [6], [4] and the ROLLERBLADER [3] and various snake-like robots [5]. In contrast to more conventional locomotion using legs or powered wheels, these systems rely on relative motion of their joints to generate net motion of the body. The joint variables or *shape* variables, are moved in cyclic patterns giving rise to periodic shape variations called *gaits*. A salient feature of these systems is the presence of multiple *nonholonomic constraints* similar to the TRIKKE.

[1]http://www.trikke.com

Fig. 1. The commercial TRIKKE.

In their work with the Roller-Racer [8], Krishnaprasad and Tsakiris showed that the primary source of propulsion for the system is the periodic motion of the steering handles. Further, they also showed that the Roller-Racer is not STLC which implies that a Roller-Racer in motion cannot be brought back to rest using the single input on the system. At £rst glance, the TRIKKE seems to have similar properties. However, the TRIKKE differs from the Roller-Racer in two salient features :

- The Roller-Racer has a vertical steering axis while the TRIKKE has a tilted steering axis and a steering arrangement more like that of a bike.
- The TRIKKE handle can be *rocked* from side to side.

Various modeling techniques have been explored for such unconventional systems. Examples include the Lagrangian reduction techniques introduced in [1] and the coordinate expressions derived using the *Levi-Civita* connection in [2]. We chose to model the dynamics of the Trikke using Lagrange D'Alembert equations, since this is an easier method to use, especially given the availability of symbolic manipulation tools.

The organization of the paper is as follows. In Section II, we present a simpli£ed model for the TRIKKE. We then present simulations and comparisons with the Roller Racer in Section III. We then show how the TRIKKE's motion can be reduced to that of the Roller Racer. We also present a new proof to effectively show the lack of STLC for the TRIKKE in Section II-D. Lastly, experimental results with a small model TRIKKE are presented in Section IV.

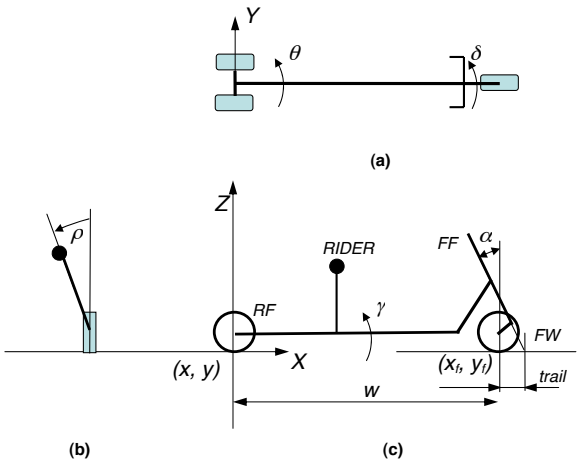

Fig. 2. The Trikke model used for analysis.

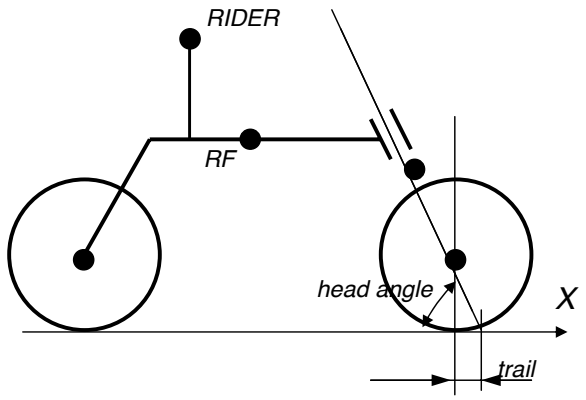

Fig. 3. A sketch of a bicycle

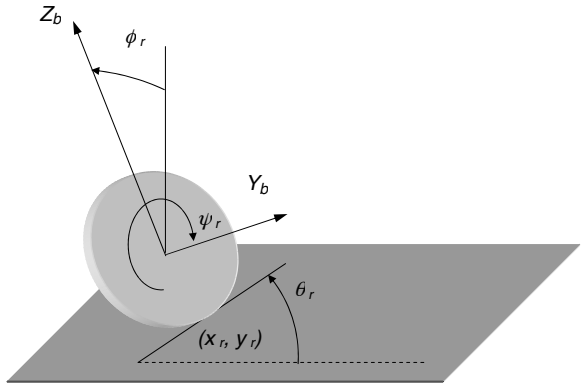

Fig. 4. A rolling, falling disc.

II. Dynamics Modeling of the Trikke System

The dynamics of the TRIKKE system are modeled using the classical Lagrange D'Alembert equations. More details on the use of these equations can be found in several textbooks (see [9] for an introduction to this method).

A. TRIKKE *parameters and modeling assumptions*

A side and top view of the model for the TRIKKE is shown in Fig. 2. The system consists of a steerable front wheel and two back wheels. When steering forward, the point of intersection of the steering axis with the ground is in front of the contact point (x_f, y_f) of the front wheel with the ground. This is similar to the steering arrangement for bicycles in Fig. 3. The steering arrangement for a bicycle helps ensure stability of the zero steering position, i.e. the position in which the steering angle $\delta = 0$, when the bicycle is moving.

To simplify the dynamic analysis of the system, we make a few assumptions. We assume that the rear platform does not roll from side to side. Further, as shown in Fig. 2, the steering handle has only one degree of freedom δ. This angle, henceforth referred to as the steering angle, is actuated using a torque τ_δ applied to the handle bars similar to that applied by a bicycle rider to turn the handlebars of a bicycle.

We divide the system into a set of four distinct rigid bodies: the rear platform, rear set of wheels (which we will model as a single component), the front frame and the front wheel. The con£guration of the rear wheel of the TRIKKE can be represented by $SE(2) \times S$. In the global frame, the position (x, y) of the TRIKKE is characterized by the position of point of contact of the rear wheel with the ground. The orientation θ of the TRIKKE is the orientation of the rear wheel with respect to an inertial reference frame. The steering angle δ is the angle through which the handle bars have been turned. The pitch γ is the pitch angle for the rear platform.

The steering axis is attached to the TRIKKE at an angle α as shown in Fig. 2. A wheel of radius R_{fw} is attached to the end of the steering axis. As the steering handle is turned, the rear platform of the TRIKKE will pitch up and down, i.e. the pitch angle of the rear platform γ is constrained by the steering angle δ. The front wheel is represented as a *rolling falling disk* (Fig. 4) with con£guration $(x_f, y_f, \theta_f, \phi_f, \psi_f)$.

We will add the rider as a £fth component to this system later in Section III-B. The rider has a single degree of freedom and is able to roll from side to side as shown in Fig 2. Further, we assume the existence of an actuator that provides the necessary torque τ_ρ for rolling the rider. Note that the rider is *absent* in all further modeling and simulation results except in Section III-B.

The complete con£guration for the TRIKKE is given by $q = (x, y, \theta, \psi_r, \gamma, \delta, x_f, y_f, \theta_f, \phi_f, \psi_f)$ where ψ_f and ψ_r represent the angular rotations of the front and rear wheels about their axles respectively.

The inertial parameters for the different components of a small model TRIKKE (Fig. 9) are given in Table I. The model of the TRIKKE now consists of a set of rotary and prismatic joints. Standard techniques (see eg the product of exponentials formulation in [9]) can now be used to derive the Lagrangian for the rigid bodies that make up the system. Let $(T_{rw}, T_{rf}, T_{ff}, T_{fw})$ and $(V_{rw}, V_{rf}, V_{ff}, V_{fw})$ represent the kinetic and potential energy of the rear wheel, rear frame, the front frame, the front wheel and the rider respectively. The total Lagrangian for the system is now given by

$$L = T_{rw} + T_{rf} + T_{ff} + T_{fw} - (V_{rw} + V_{rf} + V_{ff} + V_{fw}). \quad (1)$$

Parameter	Description	Value
w	Wheel base	26 cm
t	Trail	3 cm
α	Head Angle	72deg
Rear wheel(RW)		
R_{rw}	Radius	3 cm
m_{rw}	Mass	0.1 kg
I_{rw}	Moment of inertia about Y axis	0.012kgm^2
Rear frame (RF)		
(x_{rf}, y_{rf}, z_{rf})	Position centre of mass	$(12, 0, 8)$ cm
m_{rf}	Mass	0.5 kg
(I_{yy}, I_{zz})	Mass moment of inertia	$(0.12, 0.12)\text{kgm}^2$
Front frame (FF)		
(x_{ff}, y_{ff}, z_{ff})	Position centre of mass	$(28, 0, 7)$ cm
m_{ff}	Mass	0.15 kg
(I_{xx}, I_{yy}, I_{zz})	Moment of inertia	$(0.06, 0.06, 0.012)\text{kgm}^2$
Front wheel (FW)		
R_{fw}	Radius	0.03 m
m_{ff}	Mass	0.1 kg
(I_{xx}, I_{yy}, I_{zz})	Moments of inertia	$(0.006, 0.012, 0.006)\text{kgm}^2$
Rider		
(x_{ri}, y_{ri}, z_{ri})	Position centre of mass	$(12, 0, 12)$ cm
(x_{le}, y_{le}, z_{le})	Rider Lean/Rotary hinge position	$(12, 0, 8)$ cm
m_{ri}	Mass	0.5 kg
I_{ri}	Mass moments of inertia	0.1kgm^2

TABLE I
TRIKKE MODEL PARAMETERS.

B. Constraints

There are a total of four nonholonomic constraints acting on the system at the front and rear wheels:

$$\begin{aligned}\omega_1 &= \dot{x} + R_{rw}\dot{\psi}_r \cos\theta,\\ \omega_2 &= \dot{y} + R_{rw}\dot{\psi}_r \sin\theta,\\ \omega_3 &= \dot{x} + R_{fw}\dot{\psi}_f \cos\theta_f,\\ \omega_4 &= \dot{y} + R_{fw}\dot{\psi}_f \sin\theta_f.\end{aligned}$$

In addition the system is subject to a set of holonomic constraints that constraints some of the con£guration variables of the motion. As mentioned earlier, the pitch of the rear platform γ is constrained by the steering angle. Further, the position and orientation of the front wheel of the TRIKKE can be completely determined given the other con£guration variables. Thus, given (x, y, θ, δ), the variables $(\gamma, x_f, y_f, \theta_f, \phi_f)$ can be completely determined. These constraints take the form of algebraic equations in the con£guration variables.

A £rst set of 3 constraints is obtained by equating the position of the center of the front wheel derived through the rear frame with the position of the same point derived through the front wheel. Two further constraints can be obtained by equating the direction of the body £xed y axis of the front wheel from the two approaches. This leads to a set of £ve *holonomic* constraints of the form

$$f_i(q) = 0,\ i = 1, \ldots, 5. \tag{2}$$

C. Dynamic Equations

The £rst step in deriving the dynamic equations of the TRIKKE is to differentiate the holonomic constraints. This gives rise to a set of 5 equations linear in the velocities of the system. Combining these equations with the four nonholonomic constraints gives a set of 9 equations linear in the velocities that can be written in the form:

$$A(q)\dot{q} = 0. \tag{3}$$

Now, we choose an appropriate basis for the nullspace of $A(q)$ so that the allowable velocities for the system are given by

$$\dot{q} = \Gamma\dot{q}_d. \tag{4}$$

Here, the columns of Γ are the basis vectors for the nullspace of $A(q)$. There are 9 constraints and the con£guration space has dimension 11. Hence there exist only 2 degrees of freedom. Thus, of the 11 velocities in $\dot{q}$ we can choose only the 2 in $\dot{q}_d$ independently. We choose the basis such that the two independent velocities correspond to the angular rotation of the rear wheel of the system and the steering angle rate, ie $\dot{q}_d = (\dot{\psi}_r, \dot{\delta})$.

Now, using the Lagrange D'Alembert equations, we can write the dynamic equations of the system as,

$$\tilde{M}\ddot{q}_d + \tilde{C}(q)[\dot{q}_d, \dot{q}_d] + \tilde{N}(q, \dot{q}_d) = \tilde{\tau}. \tag{5}$$

Here,

$$\tilde{\tau} = \Gamma^T\tau = \Gamma^T \begin{bmatrix}\mathbf{0}_{5\times1}\\ \tau_\delta \\ \mathbf{0}_{5\times1}\end{bmatrix} \tag{6}$$

Here, τ_δ, the steering torque, is the only torque acting on the system. As in [2], we can also move $\tilde{M}$ to the right hand side of Equation 5 and rewrite it in a form that we will use in the next section as

$$\dot{v}_k + \tilde{\Gamma}^k_{ij}(q) = \sum_{a=1}^{m} Y^k_a u_a - V^k. \tag{7}$$

Here, $v_1 = \dot{q}_d(1)$ and $v_2 = \dot{q}_d(2)$ and $m = 1$ is the number of inputs to the system. Explicitly writing out the equations, we £nd they are of the following form

$$\begin{cases} \dot{v}_1 &= -(\tilde{\Gamma}^1_{12}(\psi) + \tilde{\Gamma}^1_{21}(\psi))v_1v_2 - \tilde{\Gamma}^1_{22}(\psi)v_2^2,\\ \dot{v}_2 &= -\tilde{\Gamma}^2_{11}(\psi)v_1^2 - \tilde{\Gamma}^2_{21}(\psi)v_1v_2 - \tilde{\Gamma}^2_{22}(\psi)v_2^2\\ &\quad + f_u(\psi)u + f_g(\psi), \end{cases} \tag{8}$$

Equations 4 and 5 represent the complete dynamics of the TRIKKE model on the reduced state space $(q, \dot{q}_d)$. Note that this approach is very similar (and equivalent) to the approach in [2].

D. Controllability analysis

In this section, we will show the following proposition based on the derivation of a global optimal control. In [8], a similar result was presented for the Roller-Racer.

Proposition 1: If, for any given ψ, $\tilde{\Gamma}^1_{22}(\psi) > 0$ in Eq. 8, then, given x_1 and x_2 in the con£guration space with $x_1 \neq x_2$, the system cannot go from rest at x_1 to rest at x_2.

To study whether the TRIKKE can be stopped, we only need to consider dynamics of v_1 and v_2 ignoring the position and orientation of the system. Furthermore, by assuming that $f_u(\psi) > 0$ for any ψ such that v_2 is fully controlled, we have the following *relaxed control problem*.

$$\begin{cases} \dot{v}_1 &= -(\tilde{\Gamma}^1_{12}(\psi) + \tilde{\Gamma}^1_{21}(\psi))v_1 v_2 - \tilde{\Gamma}^1_{22}(\psi)v_2^2, \\ \dot{\psi} &= v_2, \end{cases} \tag{9}$$

in which v_2 is considered as a control.

Remark: Any v_2 history that is obtained by applying some control u on the system in Eq. 8 is an admissible control for the relaxed problem, i.e., the set of available controls to the relaxed problem could be considered as a superset of the control set for the original problem in Eq. 8. If we show that the system in the relaxed control problem cannot be stopped if starting moving from rest, then the TRIKKE system also has this property.

To show that the system in Eq. 9 is unstoppable, we need the following lemma, which provides a global optimal control to increase the value of v_1 for the relaxed control problem in Eq. 9.

Lemma 1: For the control system in Eq. 9 starting at time 0, if $\tilde{\Gamma}^1_{22}(\psi) > 0$ for any ψ, then for any $t > 0$, $v_1(t)$ will reach its global maximal value

$$v_1^*(t) = v_1(0)e^{c(t)}, \tag{10}$$

in which

$$c(t) = \int_{\psi(0)}^{\psi(t)} \frac{\tilde{\Gamma}^1_{12}(\psi) + \tilde{\Gamma}^1_{21}(\psi)}{2} d\psi \tag{11}$$

when the control

$$v_2(t) = -\frac{\tilde{\Gamma}^1_{12}(\psi(t)) + \tilde{\Gamma}^1_{21}(\psi(t)))}{2\tilde{\Gamma}^1_{22}(\psi(t))} v_1(t). \tag{12}$$

Proof: There are two steps in the proof. We £rst show that there exists a global optimal control. In the second part, we derive the value of $v_1^*(t)$ under the optimal control.

From Eq. 9, we have

$$\begin{aligned} \delta v_1(t) &= \int_{t_0}^{t} \Big[-(\tilde{\Gamma}^1_{12}(\psi(s)) + \tilde{\Gamma}^1_{21}(\psi(s)))v_1(s)v_2(s) \\ &\quad -\tilde{\Gamma}^1_{22}(\psi(s))v_2^2(s) \Big] ds. \end{aligned} \tag{13}$$

When δv_1 reaches an extreme point under the control v_2, we have the following equality for any $t > t_0$

$$\begin{aligned} \tfrac{\partial \delta v_1}{\partial v_2} &= \int_{t_0}^{t} \Big[-(\tilde{\Gamma}^1_{12}(\psi(s)) + \tilde{\Gamma}^1_{21}(\psi(s)))v_1(s) \\ &\quad -2\tilde{\Gamma}^1_{22}((\psi(s))v_2(s) \Big] ds \\ &= 0. \end{aligned} \tag{14}$$

Therefore, when $v_2(t) = -\frac{\tilde{\Gamma}^1_{12}(\psi(t)) + \tilde{\Gamma}^1_{21}(\psi(t)))}{2\tilde{\Gamma}^1_{22}(\psi(t))} v_1(t)$ for any $t > t_0$, δv_1 will reach the only extreme point. Since $\tilde{\Gamma}^1_{22}(\psi) > 0$, such a control always exists.

Furthermore, the second partial derivative of δv_1 to v_2 is

$$\frac{\partial^2 \delta v_1}{\partial v_2^2} = \int_{t_0}^{t} -2\tilde{\Gamma}^1_{22}(\psi(s)) ds. \tag{15}$$

Since $\tilde{\Gamma}^1_{22} > 0$ for any ψ, we have $\frac{\partial^2 \delta v_1}{\partial v_2^2}$ less than 0. Therefore, when $v_2 = -\frac{a_1(\psi)}{2a_2(\psi)} v_1$, δv_1 will reach the global maximum value.

Applying the global optimal control in Eq. 12 to the system in Eq. 9, we have:

$$\begin{cases} \frac{dv_1}{dt} &= -\frac{(\tilde{\Gamma}^1_{12}(\psi) + \tilde{\Gamma}^1_{21}(\psi))^2}{4\tilde{\Gamma}^1_{22}(\psi)} v_1^2 \\ \frac{d\psi}{dt} &= -\frac{\tilde{\Gamma}^1_{12}(\psi) + \tilde{\Gamma}^1_{21}(\psi))}{2\tilde{\Gamma}^1_{22}(\psi)} v_1 \end{cases} \tag{16}$$

¿From Eq. 16, we have

$$\frac{dv_1}{v_1} = \frac{\tilde{\Gamma}^1_{12}(\psi) + \tilde{\Gamma}^1_{21}(\psi)}{2} d\psi. \tag{17}$$

By solving the above differential equation in time interval $[0, t]$, we obtain the optimal value for $v_1^*(t)$ in the lemma. □

Lemma 2: For the control system in Eq. 9, the set $\{(v_1, \psi) : v_1 \leq 0\}$ is a positively invariant set. That is, if $v_1(t_0) < 0$, then $v_1(t) < 0$, $\forall t \geq t_0$. Furthermore, $v_1(t_0) \leq 0$ and $v_1(t_f) = 0$ for some $t_f \geq t_0$, if and only if $v_1(t) = 0$, $\forall t \in [t_0, t_f]$.

Proof: According to Eq. 10, it is easy to see that if $v_1(t_0) < 0$, then the maximal $v_1^*(t) < 0$ since $e^{c(t_f)} > 0$ for any $t \geq t_0$.

We can also see that the maximal $v_1^*(t_f) = 0$ for $t_f \geq t_0$ happens if and only if when $v_1(t_0) = 0$ and control $v_2(t) = 0$ for any $t > t_0$ is applied, i.e., $v_1(t) = 0$, $\forall t \in [t_0, t_f]$. □

Proof of Proposition 1: We will £rst show that $v_1(t) < 0$ for the system if it moves away from x_1 at rest. Then, we show that there exists no control that can bring the TRIKKE to rest from $v_1 < 0$.

First, since the TRIKKE system needs to move from con£guration x_1 at rest to con£guration $x_2 \neq x_1$, some control u is necessary to change v_2 such that v_2 will not be zero all the time; otherwise, the system will keep still without moving. This is equivalent to applying a nonzero control v_2 on the system in Eq. 9. By Lemma 1, if $v_1(0) = 0$, then the optimal value $v_1^*(t) = 0$ for any $t > 0$ under the control $v_2(t) = 0$ for any $t > 0$. Therefore, if a nonzero control v_2 is applied, v_1 can only become negative.

Now, we want to know whether there exists a control u which will bring the TRIKKE to rest from a negative $v_1(t')$ for some $t' > 0$. For any control u, we have a v_2 history for the TRIKKE system, which could be considered as a control for the system in Eq. 9. From Lemma 2, we can see that there is also no such control u for the TRIKKE. □

It is easy to see that if the head angle α is changed to 0, then the TRIKKE is reduced into a roller racer since the height of the mass center will not change with respect to the variation of the steering angle. Therefore, the dynamics of the roller racer will also be in the form of Eq. 8. We have the following corollary.

Corollary 1: If, for any given ψ, $\tilde{\Gamma}^1_{22}(\psi) > 0$ in Eq. 8, then, given x_1 and x_2 in the con£guration space with $x_1 \neq x_2$, the roller racer cannot move from rest at x_1 to rest at x_2.

III. Simulation

The Trikke was simulated by applying different controls on the steering angle δ and the rider lean ρ. We focused on two particular aspects of the Trikke in simulation: the effect of steering axis tilt and rider inputs. Sinusoids were used to specify the desired trajectories for the control variables:

$$\delta_d = \delta_o + \delta_a \sin(\omega_\delta t + \phi_\delta), \tag{18}$$

$$\rho_d = \rho_o + \rho_a \sin(\omega_\rho t + \phi_\rho). \tag{19}$$

Feedback linearization can be used to obtain direct control of the input variables. Thus, using an appropriate control law, we have

$$\ddot{\delta} = u_1, \tag{20}$$

$$\ddot{\rho} = u_2, \tag{21}$$

where u_1 and u_2 are control inputs. In practice, the use of a servo motor on our robot allows us to directly specify the desired angles and thus justi£es our assumption of direct control on the input variables.

We will now present simulation results for different cases. We will also compare our results to those for a simulated Roller Racer and to actual experimental results.

A. Trikke without rider

The £rst set of simulation results are for the case where there is no rider on the Trikke. Figure 5 shows the resultant motion of the system using a sinusoid of amplitude $\delta_a = 0.9$, frequency $\omega_\delta = 1$ Hz and offset $\delta_o = 0$. As expected, the system moves forward in a sinusoidal gait. As energy is pumped into the system by the periodic input, the momentum of the system increases continuously with time.

For this particular δ_a, Fig 6 shows a comparison of the trajectories of a Trikke, a Roller-Racer and our experimental prototype. The Roller-Racer model was derived from the Trikke model by setting the steering tilt $\alpha = 0$. It can be seen that for the same input, the Trikke travels faster than the Roller-Racer. This is a consequence of the tilted steering axis of the Trikke where in the rear body of the Trikke pitches up and down affecting the dynamics of the system. The results for the experimental prototype do not match the simulated results. More details on the experiments are presented later in Section IV.

It is clear that the Roller Racer and the Trikke share the same basic method of propulsion. However, propulsion is enhanced in the Trikke by the rocking motion of the rider and the tilted steering axis.

B. Effect of rider

We also modeled the effect of a rider sitting on the Trikke and rolling from side to side. The derivation of the model for the rider requires the introduction of a new con£guration variable ρ. The rider is modeled as a rotary joint with a mass at one end that can swing from side to side. It is assumed that an actuator is present at the pivot point that allows direct control of ρ. This corresponds to the torque exerted at the hip by a human rider to swing his upper body from side to side. Figures 7 and 8 show the response of the system to 3 different inputs: (1) A zero-lean input where the rider is controlled so that $\rho = 0$, (2) In-phase inputs speci£ed as $\rho_a = \delta_a$ and $\phi_\rho = \phi_\delta = 0$ and (3) Out of phase inputs where $\rho_a = \delta_a$ and $\phi_\rho = \pi$ and $\phi_\delta = 0$.

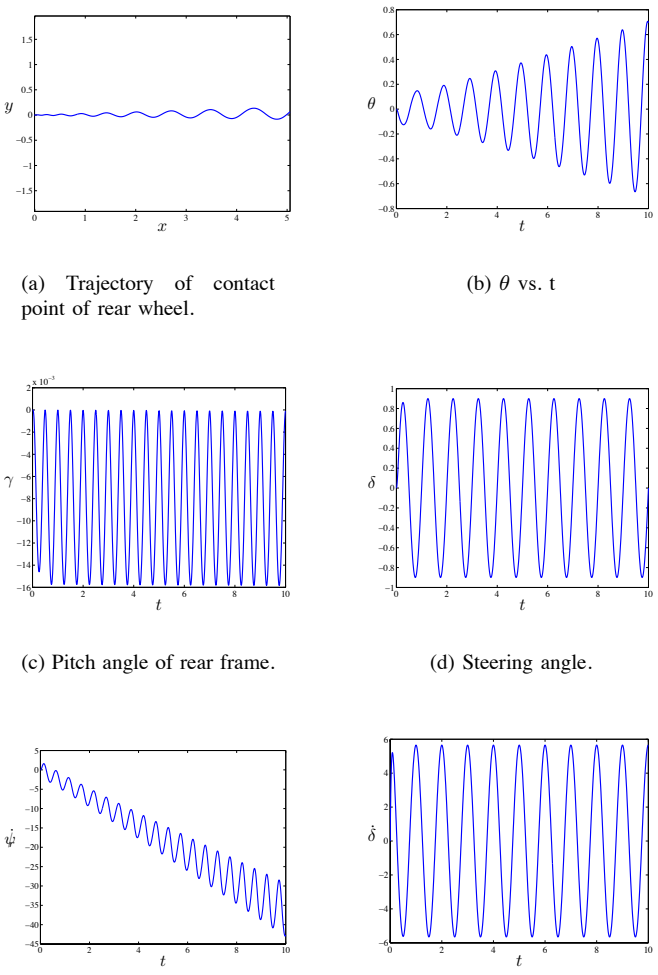

(a) Trajectory of contact point of rear wheel.

(b) θ vs. t

(c) Pitch angle of rear frame.

(d) Steering angle.

(e) Angular velocity of rear wheel.

(f) Steering angle velocity.

Fig. 5. Simulation results for sinusoidal input.

The simulations con£rm that rider input has a de£nite effect on the motion of the system. The case of in-phase inputs corresponds to the rider leaning away from the direction in which the steering handle is turned. This kind of rider input slows down the system. The out of phase motion corresponds to the rider leaning into the direction the steering handle is turned which is seen to speed up the system. This kind of behavior is exploited by human riders of the Trikke system who *rock* from side to side to impart greater momentum to their vehicles.

IV. Experimental Implementation

We now present experimental results for a small robotic model of the Trikke. We describe the experimental setup and open-loop experiments and then present closed-loop results.

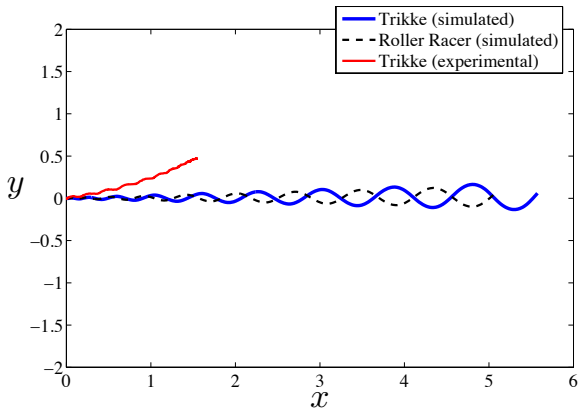

Fig. 6. Trajectory of the TRIKKE (simulated), Roller Racer (simulated) and TRIKKE (experimental).

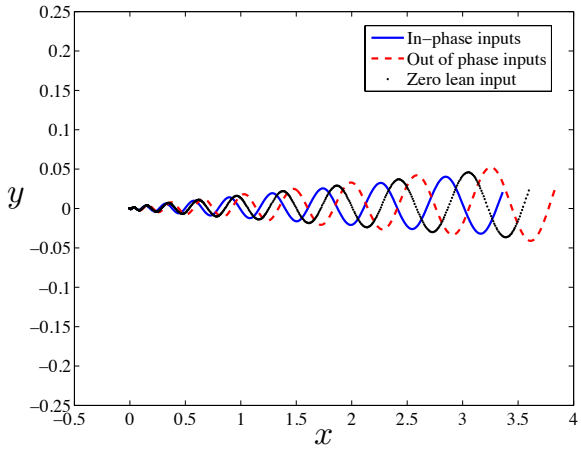

Fig. 7. Trajectory of TRIKKE for in-phase, out of phase and zero lean input.

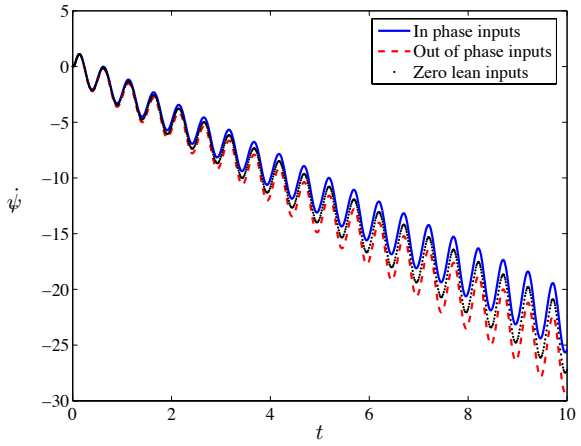

Fig. 8. Angular velocity of rear wheel for in-phase, out of phase and zero lean input.

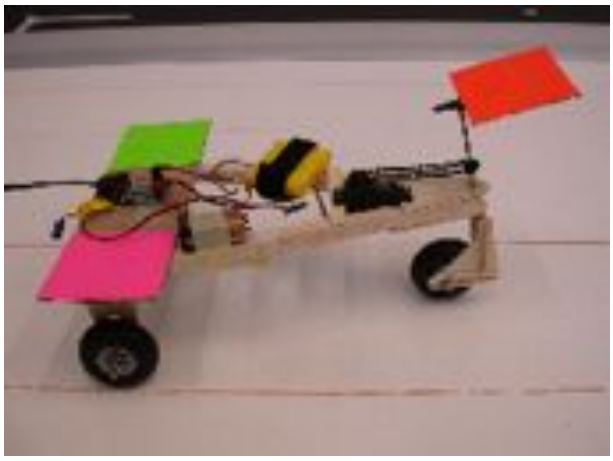

Fig. 9. A small model TRIKKE used in the experiment.

A. Model

The experiments are based on the small model TRIKKE shown in Fig. 9. The model has no rider on it, ie there is only one input present on the system - the steering angle. The model has a steering axis tilted at approximately 18 degrees. The steering angle is actuated directly using a servo. The eperiments were carried out by specifying a control for the steering angle of the form,

$$\delta_d = \delta_o + \delta_a \sin(\omega_\delta t + \phi_\delta). \tag{22}$$

The input was converted into the appropriate PWM signal for the servo and transmitted using a MINI SSC board interfaced to a laptop.

A camera based visual tracking system was used to track the motion of the robot. Three colored markers of different colors were placed on the robot and tracked using an overhead camera (Fig. 9). One of the markers was placed on the handlebars to aid in recovery of the actual values of δ. The other two markers were used to recover the position and orientation of the body of the TRIKKE. The tracking system was run at approximately 30 Hz.

B. Forward motion

In the £rst set of experiments, the amplitude of the input, δ_a, was varied while the other parameters were held constant at $(\delta_o = 0, \omega = 1 \text{ Hz}, \phi_{delta} = 0)$. The experiments were run for 10 cycles of the periodic input. The net motion of the robot was expected to be along the positive Y axis. This input leads to forward motion of the TRIKKE. Experimental trajectories are shown in Fig. 10(a). In Fig. 10(b), d_s is the actual distance traveled by the system along its path, while Fig. 10(c) plots x_f, the amount by which the £nal position of the system is offset laterally from the y axis. Representative results for one particular trajectory are shown in Figures 11(a) to 11(c).

C. Moving on a curve

Using an offset to the sinusoidal inputs used earlier, we can get the TRIKKE to move along a curve. We choose the constant parameters $(\delta_a = 1, \omega = 1 \text{ Hz}, \phi_d elta = 0)$ and vary δ_o from -0.5 to 0.5. Experimental trajectories for this set of experiments are shown in 12(a). The variation of the £nal

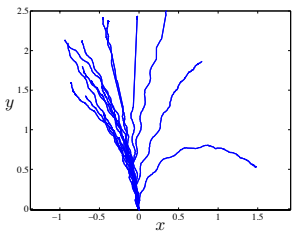

(a) Experimental trajectories of the TRIKKE for different δ_a.

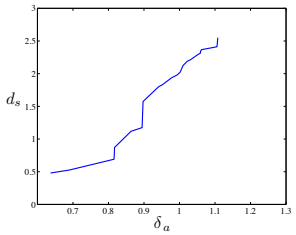

(b) Distance traveled along the path of the TRIKKE.

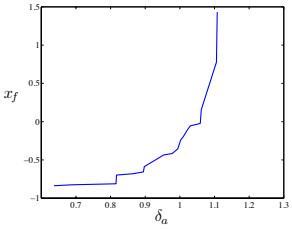

(c) Lateral deviation of TRIKKE at the end of 10 cycles

Fig. 10. Open-loop experiments for forward motion.

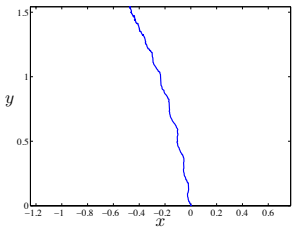

(a) Forward motion of TRIKKE for δ_a = 0.9.

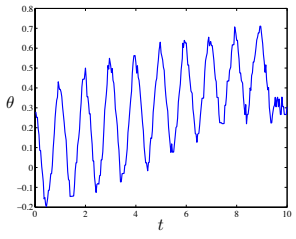

(b) Orientation of the TRIKKE vs t for δ_a = 0.9.

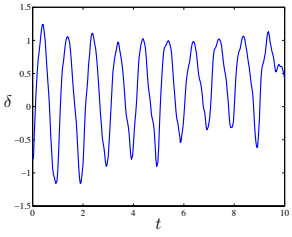

(c) Variation of δ for δ_a = 0.9.

Fig. 11. Motion of the TRIKKE for zero-offset sinusoidal input.

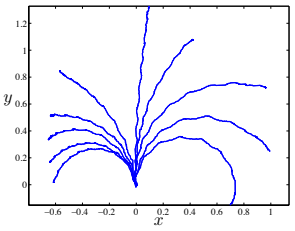

(a) Experimental curved trajectories of the TRIKKE for different offsets δ_o.

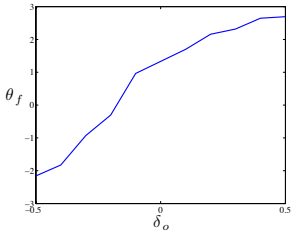

(b) Final orientation of the TRIKKE for different offsets.

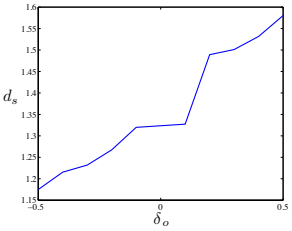

(c) Distance traveled along the path of the TRIKKE.

Fig. 12. Open-loop turning experiments for the TRIKKE

orientation of the TRIKKE after 10 cycles of periodic input is shown in 12(b) while the distance traveled along the curve is shown in 12(c).

D. Closed loop control

Using the visual tracking system, we were able to get feedback for the position and orientation of the TRIKKE. Using this information and the experimental results and observations from the open-loop control of the system, we attempted to carry out closed loop control of the TRIKKE. Note that, as proven earlier, the TRIKKE cannot be stopped. The work of stopping the TRIKKE in experiments is done by friction.

Using the fact that the system starts rotating when the input is offset, we developed a simple feedback control law. From the open loop control experiments, we had observed the variation of turn angle rate with δ_o. This helped us tune the gains for the controller. The desired trajectory for the system was specified as motion along y_d = constant = 6.25 with respect to a global inertial frame. The control input is the same as the one in IV-A. The amplitude of the commanded input gait for δ was fixed, ie $\delta_a = constant = 1.0$. Thus, the only parameter that was varied was the input offset δ_o. The other parameters for the gait are $\omega_\delta = 1$ Hz.

The control law chosen to drive the system is given by:

$$\delta_o = K_p(y_d - y) - K_d\dot{y}. \tag{23}$$

However, the velocity data $\dot{y}$ required for feedback was noisy and inaccurate. Hence, we modified the feedback law to the following form

$$\delta_o = K_p(y_d - y) - K_{d2}\sin\theta. \tag{24}$$

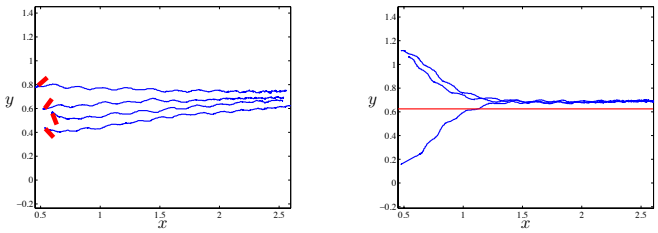

(a) Non-zero starting orientations θ indicated by red lines.

(b) Starting orientations $\theta = 0$.

Fig. 13. Closed loop control to y_d = constant = 6.25.

The controller updates the desired offset angle δ_o at 4 Hz. Experimental results for two different sets of runs are shown in Figures 13(a) and 13(b). In the £rst set of runs (Fig. 13(a)), the system starts from a non-zero initial orientation. In the second set of runs (Fig. 13(b)), the system started from a zero orientation but with a larger offset in the Y direction.

E. Discussion of experimental results

The quantitative behavior of the real TRIKKE does not match the simulated system. There are several reasons for this. Friction plays a big part in slowing down the motion of the real robot. Further, the inertia parameters chosen for simulation may not match the real parameters. Slipping was observed at the wheels of the real TRIKKE. The real model was also observed to be biased towards one side. Errors in calibration of the actuator also play a big part in the deviation from ideal behavior. Disturbances like a gentle upward slope or a small crack in the surface also contributed to the deviation from simulated behavior. Actuator limitations also played a part in the observed differences.

As can be seen from the closed-loop experiments, the TRIKKE under control performed reasonably well. The system was able to correct for fairly large lateral and orientation deviations. Because of limited workspace and the limited £eld of view of the camera, the robot frequently reached the limits of the workspace before it could converge to the desired trajectory. This also contributed to the errors in the lateral position of the robot under closed-loop control. Visual feedback from the camera was also signi£cantly affected by lighting conditions.

V. CONCLUSION

In this paper, we model the dynamics of the TRIKKE system. We show that the TRIKKE shares a common propulsive method with the Roller Racer that is enhanced by the difference in their geometry. Based on a global optimal control, we prove that the trikke and the roller racer, with only one control, cannot be stopped if they start from the rest. Experiments with a simpli£ed robot model justify our modeling and analysis results. We have also carried out closed-loop control for the robotic model using visual feedback and executed a simple control law to converge onto a straight line.

In the future, we would like to explore the use of randomized trajectory planning methods for such systems. We also plan to add an extra degree of freedom to our robot to more closely match the degrees of freedom in the actual TRIKKE. In particular, we would like to explore experimentally the effect of the rider on the system.

VI. ACKNOWLEDGMENTS

The authors would like to thank Prof. Francesco Bullo for his thoughtful comments and notes. The authors would also like to thank Geoff Bower for building the model of the TRIKKE. This research is partially supported by NSF grant CCR-0133869.

REFERENCES

[1] A. M. Bloch, P. S. Krishnaprasad, J. E. Marsden, and R. M. Murray. Nonholonomic mechanical systems with symmetry. *Archive for Rational Mechanics and Analysis*, 136(1):21–99, 1996.

[2] Francesco Bullo and Milos Zefran. On mechanical control systems with nonholonomic constraints and symmetries. *Systems and Control Letters*, 45(2):133–143, 2002.

[3] Sachin Chitta, Frederik Heger, and Vijay Kumar. Design and gait control of a rollerblading robot. In *Proc. IEEE Intl. Conf. on Robotics and Automation*, New Orleans, April 2004.

[4] Gen Endo and Shigeo Hirose. Study on Roller-Walker : Multi-mode steering control and self-contained locomotion. In *Proc. IEEE Int. Conf. Robotics and Automation*, pages 2808–2814, San Francisco, April 2000.

[5] S. Hirose and A. Morishima. Design and control of a mobile robot with an articulated body. *The International Journal of Robotics Research*, 9(2):99–114, 1990.

[6] Shigeo Hirose and Hiroki Takeuchi. Study on Roller-Walker (Basic Characteristics and its Control). In *Proc. IEEE Int. Conf. Robotics and Automation*, pages 3265–3270, Minneapolis, 1996.

[7] P. S. Krishnaprasad and D. P. Tsakiris. G-snakes: Nonholonomic kinematic chains on lie groups. In *Proc. 33rd IEEE Conf. on Decision and Control*, Buena Vista, FL, 1994.

[8] P. S. Krishnaprasad and D. P. Tsakiris. Oscillations, SE(2)-Snakes and Motion Control: A Study of the Roller Racer. Technical report, Center for Dynamics and Control of Smart Structures (CDCSS), University of Maryland, College Park, 1998.

[9] Richard M. Murray, Zexiang Li, and S. Shankar Sastry. *A Mathematical Introduction to Robotic Manipulation*. CRC, 1993.

[10] James P. Ostrowski. *The Mechanics and Control of Undulatory Robotic Locomotion*. PhD thesis, California Institute of Technology, Pasadena, CA, 1995.